



## Discrimination of Textures using Texton Patterns

By Shaik Rahamat Basha & P Kiran Kumar Reddy

*Narayana Engineering College, Gudur, India*

**Abstract-** Textural patterns can often be used to recognize familiar objects in an image or retrieve images with similar texture from a database. Texture patterns can provide significant and abundance of texture and shape information. One of the recent significant and important texture features called Texton represents the various patterns of image which is useful in texture analysis. The present paper is an extension of our previous paper [1]. The present paper divides the  $3 \times 3$  neighbourhood into two different  $2 \times 2$  neighbourhood grids each consist four pixels. On this  $2 \times 2$  grids shape descriptor indexes (SDI) are evaluated separately and added to form a Total Shape Descriptor Index Image (TSDI). By deriving textons on TSDI image Total Texton Shape Matrix (TTSM) image is formed and Grey Level Co-Occurrence Matrix (GLCM) parameters are derived on it for efficient texture discrimination. The experimental result shows the efficacy of the present method.

**Keyword:** *textons, glcm features, shape descriptor index (sdi), total shape descriptor index image (tsdi). total texton shape matrix (ttsm),  $2 \times 2$  grids.*

**GJCST-F Classification:** *1.2.10*



*Strictly as per the compliance and regulations of:*



# Discrimination of Textures using Texton Patterns

Shaik Rahamat Basha <sup>α</sup> & P Kiran Kumar Reddy <sup>ο</sup>

**Abstract-** Textural patterns can often be used to recognize familiar objects in an image or retrieve images with similar texture from a database. Texture patterns can provide significant and abundance of texture and shape information. One of the recent significant and important texture features called Texton represents the various patterns of image which is useful in texture analysis. The present paper is an extension of our previous paper [1]. The present paper divides the  $3 \times 3$  neighbourhood into two different  $2 \times 2$  neighbourhood grids each consist four pixels. On this  $2 \times 2$  grids shape descriptor indexes (SDI) are evaluated separately and added to form a Total Shape Descriptor Index Image (TSDI). By deriving textons on TSDI image Total Texton Shape Matrix (TTSM) image is formed and Grey Level Co-Occurrence Matrix (GLCM) parameters are derived on it for efficient texture discrimination. The experimental result shows the efficacy of the present method.

**Keywords:** *textons, glcm features, shape descriptor index (sdi), total shape descriptor index image (tsdi), total texton shape matrix (ttsm),  $2 \times 2$  grids.*

## I. INTRODUCTION

Analysis of texture requires the identification of proper attributes or features that differentiate the textures in the image for segmentation, classification and recognition. Initially, texture analysis was based on the first order or second order statistics of textures [6, 7, 8, 9, 10]. Then, Gaussian Markov random field (GMRF) and Gibbs random field models were proposed to characterize textures [11, 12, 13, 14, 15, 16]. Later, local linear transformations are used to compute texture features [17, 18]. Then, texture spectrum technique was proposed for texture analysis [19]. The above traditional statistical approaches to texture analysis, such as co-occurrence matrices, second order statistics, GMRF, local linear transforms and texture spectrum are restricted to the analysis of spatial interactions over relatively small neighborhoods on a single scale. As a consequence, their performance is best for the analysis of micro textures only [20]. More recently, methods based on multi-resolution or multi-channel analysis, such as Gabor filters and wavelet transform, have received a lot of attention [21, 22, 23, 24, 25, 26, 27, 23, 25]. From the literature survey, the present study found the Gray Level Co-occurrence

Matrix (GLCM) is a benchmark method for extracting Haralick features (angular second moment, contrast, correlation, variance, inverse difference moment, sum average, sum variance, sum entropy, entropy, difference variance, difference entropy, information measures of correlation and maximal correlation coefficient) or Conners features [28] (inertia, cluster shade, cluster prominence, local homogeneity, energy and entropy). These features have been widely used in the analysis, classification and interpretation of remotely sensed data. Its aim is to characterize the stochastic properties of the spatial distribution of grey levels in an image.

The present paper is organized as follows. In the second section we have given clear information about grey level co-occurrence matrix information and the third section we discussed about textons. In fourth section we discussed deriving different Shape Descriptor Indexes (SDI). In the fifth section, proposed methodology is discussed and in sixth section results and discussions are given. Finally in last section we concluded about this paper.

## II. GRAY LEVEL CO-OCCURRENCE MATRIX

One of the other most popular statistical methods used to measure the textural information of images is the Gray Level Co-occurrence Matrix (GLCM). The GLCM method gives reasonable texture information of an image that can be obtained only from two pixels. Grey level co-occurrence matrices introduced by Haralick [29] attempt to describe texture by statistically sampling how certain grey levels occur in relation to other grey levels. Suppose an image to be analyzed is rectangular and has  $N_x$  rows and  $N_y$  columns. Assume that the gray level appearing at each pixel is quantized to  $N_g$  levels. Let  $L_x = \{1, 2, \dots, N_x\}$  be the horizontal spatial domain,  $L_y = \{1, 2, \dots, N_y\}$  be the vertical spatial domain, and  $G = \{0, 1, 2, \dots, N_g - 1\}$  be the set of  $N_g$  quantized gray levels. The set  $L_x \times L_y$  is the set of pixels of the image ordered by their row-column designations. Then the image  $I$  can be represented as a function of co-occurrence matrix that assigns some gray level in  $L_x \times L_y$ ;  $I: L_x \times L_y \rightarrow G$ . The gray level transitions are calculated based on the parameters, displacement ( $d$ ) and angular orientation ( $\theta$ ). By using a  $d$  distance of one pixel and angles quantized to  $45^\circ$  intervals, four matrices of horizontal, first diagonal, vertical, and second diagonal ( $0^\circ$ ,  $45^\circ$ ,  $90^\circ$  and  $135^\circ$  degrees) are used. Then

**Author <sup>α</sup> :** Assistant Professor, Department of Information Technology, RGM CET, Nandyal, A.P, INDIA. e-mail: basha.ste@gmail.com

**Author <sup>ο</sup> :** Professor, Department of CSE, Narayana Engineering College, Gudur, A.P, INDIA. e-mail: Kiran.penubaka@gmail.com

the un-normalized frequency in the four principal directions is defined by Equation (1).

$$\left\{ \begin{array}{l} p(i, j, d, \theta) = \# \\ ((k, l), (m, n)) \in | (L_x \times L_x) \times (L_x \times L_x) | \\ (k - m = 0, |l - n| = d) \text{ or } (k - m = d, l - n = -d) \\ \text{or } (k - m = -d, l - n = d) \text{ or } (|k - m| = d, l - n = 0) \\ \text{or } (k - m = d, l - n = d) \text{ or } (|k - m| = -d, l - n = -d) \\ I(k, l) = i, I(m, n) = j \end{array} \right. \quad (1)$$

where # is the number of elements in the set, (k, l) the coordinates with gray level i, (m, n) the coordinates with gray level j. The following Fig. 1 illustrates the above definitions of a co-occurrence matrix (d=1, θ = 0°).

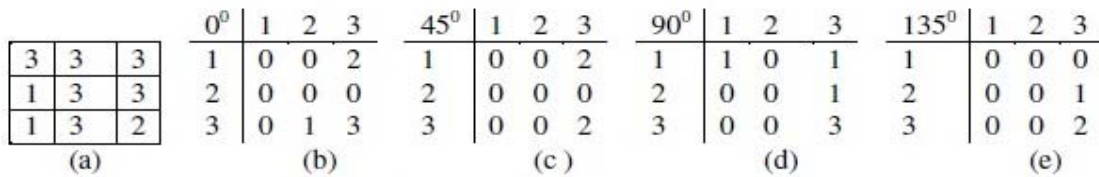


Figure 1: An example of Gray level co-occurrence matrix

Even though Haralick extracted 24 parameters from co-occurrence matrix, the present paper used only energy, contrast, local homogeneity, and correlation as given in Equations (2) to (5).

$$\text{Energy} = \sum_{i,j=0}^{N-1} -\ln(P_{ij})^2 \quad (2)$$

Energy measures the number of repeated pairs and also measures uniformity of the normalized matrix.

$$\text{Contrast} = \sum_{i,j=0}^{N-1} -P_{ij} (i - j)^2 \quad (3)$$

The contrast feature is a difference moment of the P matrix and is a standard measurement of the amount of local variations present in an image. The higher the value of contrast are, the sharper the structural variations in the image.

$$\text{Local Homogeneity} = \sum_{i,j=0}^{N-1} \left( \frac{P_{ij}}{1+(i-j)^2} \right) \quad (4)$$

It measures the closeness of the distribution of elements in the GLCM to the GLCM diagonal. The converse of homogeneity results in the statement of contrast.

$$\text{Correlation} = \sum_{i,j=0}^{N-1} \left( P_{ij} \frac{(i-\mu)(j-\mu)}{(\sigma)^2} \right) \quad (5)$$

Where  $P_{ij}$  is the pixel value in position (i, j) of the texture image, N is the number of gray levels in the image,  $\mu$  is  $\mu = \sum_{i,j=0}^{N-1} iP_{ij}$  mean of the texture image and  $(\sigma)^2$  is  $(\sigma)^2 = \sum_{i,j=0}^{N-1} P_{ij} (i - \mu)^2$  variance of the texture image. Correlation is the measure of similarity

between two images in comparison. The measures mean (m), which represents the average intensity.

### III. TEXTONS

Textons [30, 31] are considered as texture primitives, which are located with certain placement rules. A close relationship can be obtained with image features such as shape, pattern, local distribution orientation, spatial distribution, etc. using textons. The textons are defined as a set of blobs or emergent patterns sharing a common property all over the image. The different textons may form various image features. To have a precise and accurate texture classification, the present study strongly believes that one need to consider all different textons. That is the reason the present study considered all. There are several issues related with i) texton size ii) tonal difference between the size of neighbouring pixels iii) texton categories iv) expansion of textons in one orientation v) elongated elements of textons. By this sometimes a fine or coarse or an obvious shape may results or a pre-attentive discrimination is reduced or texton gradients at the texture boundaries may be increased. The present paper utilized the following five texton shades of 2x2 grid shown in Fig. 2. In Fig. 2 (a), the pixels are represented as  $d_1, d_2, d_3$  and  $d_4$ . The present paper considered texton shades if three or more pixels have the same intensity levels. This rule derives five texton shapes denoted as  $T_1, T_2, T_3, T_4$  and  $T_5$  as shown in Fig.2.

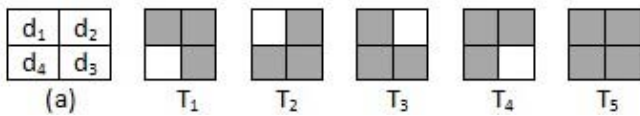


Figure 2 : Proposed 2x2 grid textons

#### IV. DERIVING DIFFERENT SHAPE DESCRIPTOR INDEXES (SDI)

Hole shape (Index = 0): The TU with 0 represents a hole shape. The hole shape consists all 0's as shown in the Fig.3.



Figure 3 : Hole shape with SDI value 0

Dot shape (Index = 1): The TU with 1, 2, 4 and 8 represents a dot shape. The dot shape will have only a single 1 as shown in Fig.4.

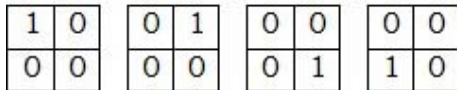
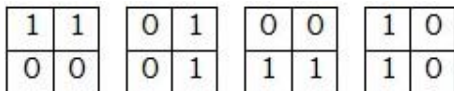


Figure 4 : The four dot shapes with SDI value 1

Horizontal/Vertical line shape (Index = 2): The two adjacent 1's results four different TU weights i.e. 3, 6, 9 and 12 and all of them represents a horizontal or vertical line as shown in Fig.5.



Diagonal Line shape (Index= 3): The other two adjacent 1's with TU values 5 and 10 represents diagonal lines as shown in Fig.6.

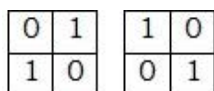


Figure 6 : Representation of diagonal line with SDI value 3

Triangle shape (Index = 4): The three adjacent 1's with TU values 7, 11, 13 and 14 represents triangle shape as shown in Fig.7.

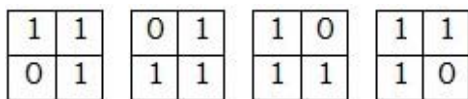


Figure 7 : Representation of triangle shape with SDI value 4

Blob shape (Index =5): TU 15 with all 1's represents a blob shape as shown in Fig.8.

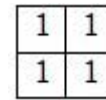


Figure 8 : Representation of blob shape with SDI value 5

The advantage of SDI is they don't depend on relative order of texture unit weights and can be given in any of the four forms as shown in Fig.9 where the relative TU will change, but shape remains the same.

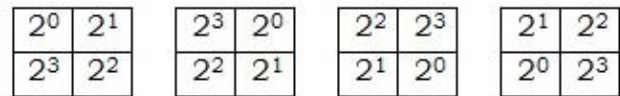


Figure 9 : Four different ways of assigning weights to TU

#### V. DERIVATION OF TOTAL TEXTON SHAPE CO-OCCURRENCE MATRIX (TTSCM)

If the given image is colour convert into gray level image. Divide each 3x3 window into two separate units by comparing neighbouring pixel value with the centre pixel as shown in fig.10 for deriving Binary Cross Texture Unit Element (BCTUE) and Binary Diagonal Texture Unit Element (BDTUE)[2,3,4,5]. As shown in Fig. 10(a) a 3x3 neighbourhood will have 8 neighbouring pixels and are divided into two sets of cross and diagonal sets with four pixels of binary values as shown in Fig.10(b & c), by following the equation 6. Represent BCTUE and BDTUE in the form of two separate 2x2 grids as shown in Fig.11.

$$b_i = \begin{cases} 0 & \text{if } S(P_c - P_i) < 0 \\ 1 & \text{if } S(P_c - P_i) \geq 0 \end{cases} \quad (6)$$

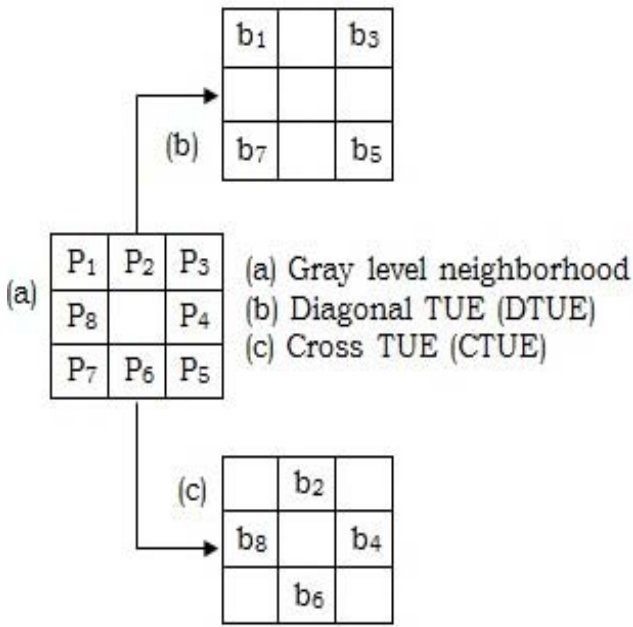


Figure 10 : Representation of 3×3 neighborhood and its BDTUE and BCTUE

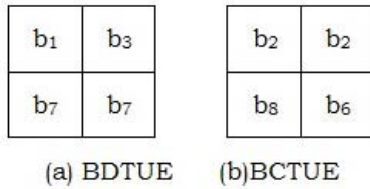


Figure 11 : Representation of 2×2 grid BDTUE and BCTUE

Derive Shape Descriptor Indexes (SDI) on BDTUE and BCTUE for deriving Diagonal SDI (DSDI) and Cross SDI (CSDI) is as shown in Fig.12 and Fig.13.

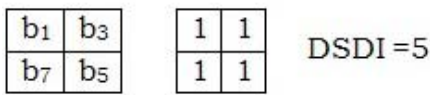


Figure 12 : BDTUE in the form 2×2 grid and derived DSDI

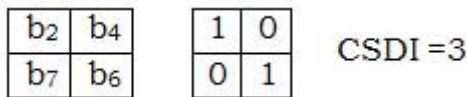


Figure 13 : BCTUE in the form 2×2 grid and derived CSDI

Repeating above process on entire image by convolving in an overlapped manner forms two separate images namely Cross Shape Descriptor Index (CSDI) and Diagonal Shape Descriptor Index (DSDI). SDI on a 2 × 2 grid ranges from 0 to 5 therefore the pixel grey level values of CSDI and DSDI images ranges from 0 to 5 only.

For forming Total Shape Descriptor Index (TSDI) image add CSDI and DSDI images as shown in Fig.14 and the pixel grey level values of TSDI image ranges from 0 to 10. Now derive textons on TSDI to form Total Texton Shape Matrix (TTSM ) image. Finally construct co-occurrence matrix on TTSM that which leads to the formation of Total Texton Shape co-occurrence Matrix (TTSCM) on which GLCM features with 0°, 45°, 90°, and 135° are derived. For efficient discrimination algorithm is derived based on the feature set values of TTSCM.

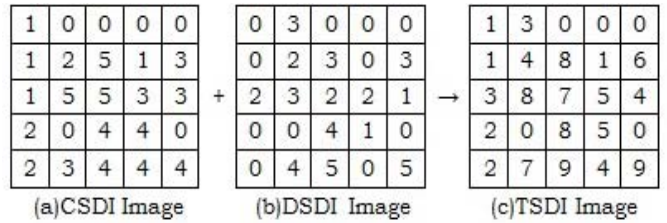


Figure 14 : Formation mechanism of TSDI image

The Fig.15, 16 and 17 represents TSDI for Car, Water and Elephant images respectively.



Figure 15 : (a) Car image (b) TSDI of (a)

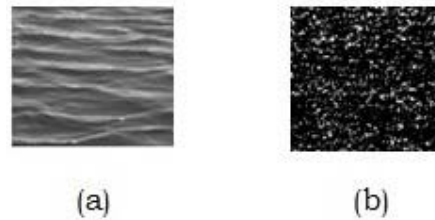


Figure 16 : (a) Water image (b) TSDI of (a)



Figure 17 : (a) Elephant image (b) TSDI of (a)

## VI. RESULTS AND DISCUSSIONS

The average of contrast, correlation, energy and homogeneity features set values on TTSCM are evaluated with a distance of one and with an orientation of 0°,45°,90° and 135° are tabulated in Table 1, 2 and 3 for the Car, Elephant and Water texture images collected

from Google data base respectively. A sample texture images of Car, Water and Elephant are shown in Fig.18. Based on feature set values of TTSCM images, Algorithm 1 is derived. Discrimination results are tabulated in Table 4 along with a bar graph shown in Fig.19. The Table 5 compares discrimination rates of our earlier methods Texton based Cross Shape Descriptor Index (TCSDI) Texton based Diagonal Shape Descriptor Index (TDSDI) [ 2,4 ] with the current method TTSCM approach of this paper. The corresponding bar graph representation is shown in Fig.20.

The proposed TTSCM obtained high discrimination rate over our earlier TCSDI and TDSDI methods. This is because the TTSCM represent the SDI of the entire image instead of two separate or partial images of TCSDI and TDSDI.



Figure 18 : Images of car, water and Eeephant textures

Table 1: Average GLCM feature values with 0°, 45°, 90° and 135° for TTSCM of Car images

Texture number	Contrast	Correlation	Energy	Homogeneity
C_1	12.655	0.5969	0.174	0.6707
C_2	13.326	0.5751	0.128	0.6317
C_3	12.499	0.6052	0.162	0.6671
C_4	11.465	0.6269	0.188	0.6838
C_5	14.144	0.5386	0.112	0.6081
C_6	13.939	0.5388	0.081	0.5848
C_7	13.542	0.5639	0.117	0.6208
C_8	13.812	0.5804	0.115	0.6377
C_9	14.126	0.5469	0.122	0.6269
C_10	11.662	0.6075	0.235	0.7022

Table 2 : Average GLCM feature values with 0°, 45°, 90° and 135° for TTSCM of Elephant images

Texture number	Contrast	Correlation	Energy	Homogeneity
E 1	9.159	0.3525	0.032	0.4971
E 2	9.809	0.3369	0.0354	0.5044
E 3	9.129	0.3472	0.0375	0.5137
E 4	9.268	0.3631	0.0375	0.5165
E 5	8.801	0.3546	0.0387	0.5187
E 6	9.187	0.3343	0.0371	0.5156
E 7	7.254	0.2813	0.0474	0.5335
E 8	6.479	0.2645	0.0509	0.5414
E 9	12.69	0.4056	0.0324	0.5063
E 10	6.252	0.2921	0.0495	0.5478

Table 3 : Average GLCM feature values with 0°, 45°, 90° and 135° for TTSCM of Water images

Texture number	Contrast	Correlation	Energy	Homogeneity
W 1	18.74	0.4686	0.0402	0.5306
W 2	16.83	0.3171	0.0327	0.4965
W 3	15.08	0.328	0.0352	0.5022
W 4	17.71	0.3615	0.0345	0.4859
W 5	18.45	0.4389	0.0301	0.5002
W 6	12.03	0.314	0.0359	0.5031
W 7	16.48	0.4387	0.0317	0.5013
W 8	15.26	0.5095	0.0408	0.5462
W 9	16.43	0.3591	0.0316	0.5024
W 10	19.39	0.3411	0.027	0.4851

Algorithm 1: Discrimination algorithm using the proposed TTSCM method.

```

Begin
if contrast >=1 && contrast <=10
    Print "Texture image is Elephant"
else if contrast > 10 && contrast <=15
    Print "Texture image is Car"
else if contrast > 15 && contrast <=20
    Print "Texture image is Water"
End
    
```

Table 4 : Discrimination rates of the proposed TTSCM method

Texture Database	Discrimination rate (%) TTSCM method
Elephant	93
Car	100
Water	86
Average Discrimination rate	93

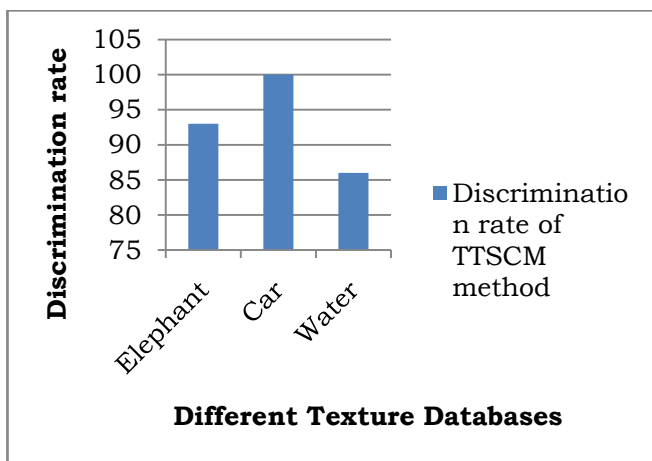


Figure 19 : Bar graph representation for Discrimination rates

Table 5 : Discrimination rates of the earlier and proposed method

Methods	Average discrimination rates (%)
TCSDI	84.33
TDSDI	88.66
TTSCM	93

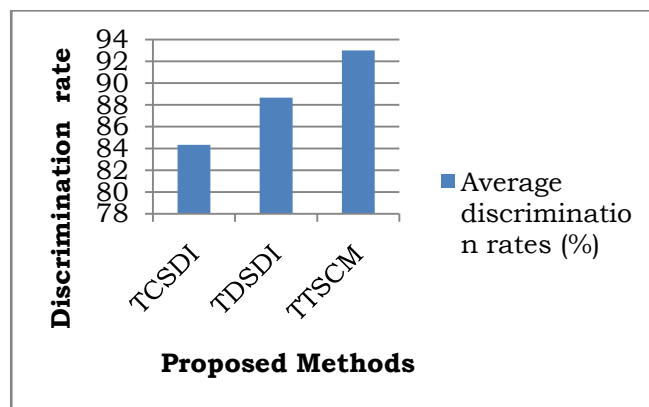


Figure 20 : Bar graph representation of proposed methods

## VII. CONCLUSION

The present paper derived TTSCM image by adding CSDI and DSDI images. By this TTSCM captured all local shape features. The present paper compared the discrimination rates of TCSDI, TDSDI and TTSCM approaches. The results clearly indicate the high discrimination rates of TTSCM over our earlier TCSDI and TDSDI methods. The TSDI represents efficient border without any disturbances when compared to CSDI and DSDI images. This is because TTSCM forms only one SDI image on the original image instead of two different SDI namely, i) TCSDI ii) TDSDI. The intensity values of TSDI image range from 0 to 10. Moreover TTSCM reduces the formation of two GLCM on the original image one representing the cross and other representing the diagonal features.

## REFERENCES RÉFÉRENCES REFERENCIAS

1. P. Kiran Kumar Reddy, B. Eswara Reddy, "Wavelet based Texton Cross and Diagonal Shape Descriptors for Discrimination of Texture", International Journal of Digital Signal and Image Processing (IJDSIP) Vol. 2, No. 3 (September 2014), pp 11-26.
2. P. Kiran Kumar Reddy, B. Eswar Reddy, "Texture Classification based on Binary Cross Diagonal Shape Descriptor Texture Matrix (BCDSDTM)", GVIP Journal, ISSN 1687-398X, Volume 14, Issue 1, August 2014, pp 45-51.
3. P. Kiran Kumar Reddy, B. Eswara Reddy, "Wavelet based Shape Descriptors using Morphology for Texture Classification", Global journal of Computer Science and Technology (GJCST) Volume XIV Issue I Version I, pp 21-27.
4. P. Kiran Kumar Reddy, V. V. Kumar, "Texture Classification Based on Cross and Diagonal Shape Descriptor Co-occurrence Matrix", CiiT International

- Journal of Digital Image Processing, Vol 6, No 06, June-July 2014, pp 261-268.
5. P. Kiran Kumar Reddy, "Derivation of Shape Descriptors on Uniform Local Binary Patterns for Classification of Textures", *IJREAT International Journal of Research in Engineering & Advanced Technology*, Volume 3, Issue 3, June-July, 2015, pp 12-22.
  6. Chen, P.C., Pavlidis, T. "Segmentation by texture using correlation". *IEEE Trans. Pattern Anal. PAMI-5*, 1983, 64– 69.
  7. Davis, L.S., Johns, S.A., Aggarwal, J.K., "Texture analysis using generalized co-occurrence matrices". *IEEE Trans. Pattern Anal. PAMI-1*, 1979, 251–259.
  8. Faugeras, O.D., Pratt, W.K., "Decorrelation methods of texture feature extraction". *IEEE Trans. Pattern Anal. PAMI-1*, 1980, 323–332 .
  9. Haralick, R.M., Shanmugam, K.K., Dinstein, I., "Texture features for image classification". *IEEE Trans. Syst. Man Cyb.* 8 (6), 1973, 610–621.
  10. Weszka, J.S., Dyer, C.R., Rosenfeld, A., "A comparative study of texture measures for terrain classification". *IEEE Trans. Syst. Man Cyb. SMC-6* (4), 1976, 269–286.
  11. Chellappa, R., Chatterjee, S., "Classification of textures using Gaussian Markov random fields". *IEEE Trans. Acoust., Speech, Signal Process. ASSP-33* (4), 1986, 959–963.
  12. Cohen, F.S., Fan, Z., Patel, M.A., "Classification of rotation and scaled textured images using Gaussian Markov random field models". *IEEE Trans. Pattern Anal.* 13 (2), 1991, 192–202.
  13. Cross, G.R., Jain, A.K., "Markov random field texture models". *IEEE Trans. Pattern Anal. PAMI- 5* (1), 1983, 25–39.
  14. Kashyap, R.L., Khotanzed, A., "A model based method for rotation invariant texture classification". *IEEE Trans. Pattern Anal. PAMI-8* (4), 1986, 472–481.
  15. Manjunath, B.S., Chellappa, R., "Unsupervised texture segmentation using Markov random fields". *IEEE Trans. Pattern Anal.* 13, 1991, 478–482.
  16. Raghu, P.P., Yegnanarayana, B., "Segmentation of Gabor filtered textures using deterministic relaxation". *IEEE Trans. Image Process.* 5 (12), 1996, 1625–1636.
  17. Laws, K.L., Rapid texture identification. *Proc. SPIE* 238, 1980, 376–380.
  18. Unser, M., "Local linear transforms for texture measurements". *Signal Process.* 11, 1986, 61–79.
  19. He, D.-C., Wang, L., "Texture unit, texture spectrum, and texture analysis". *IEEE Trans. Geo-Sci. Remote Sens.* 28 (1), 1990, 509–513.
  20. Unser, M., "Texture classification and segmentation using wavelet frames". *IEEE Trans. Image Process.* 4 (11), 1995, 1549–1560.
  21. Bovik, A., Clark, M., Geisler, W.S., "Multichannel texture analysis using localized spatial filters". *IEEE Trans. Pattern Anal.* 12, 1992, 55–73.
  22. Chang, T., Jay Kuo, C.C., "Texture analysis and classification with tree-structured wavelet transform". *IEEE Trans. Image Process.* 2 (4), 193, 429–440.
  23. Haley, G.M., Manjunath, B.S., "Rotation invariant texture classification using modified Gabor filters". *Proc. IEEE Transacitons*, 1995, 262–265.
  24. Manjunath, B.S., Ma, W.Y., "Texture features for browsing and retrieval of image data". *IEEE Trans. Pattern Anal.* 18 (8), 1996, 837–842.
  25. Raghu, P.P., Yegnanarayana, B., "Segmentation of Gabor filtered textures using deterministic relaxation". *IEEE Trans. Image Process.* 5 (12), 1996, 1625–1636.
  26. Unser, M., "Texture classification and segmentation using wavelet frames". *IEEE Trans. Image Process.* 4 (11), 1995, 1549–1560.
  27. Unser, M., Eden, M., "Multiresolution feature extraction and selection for texture segmentation". *IEEE Trans. Pattern Anal.* 2, 1989, 717–728.
  28. Kaplan, L.M., "Extended fractal analysis for texture classification and segmentation". *IEEE Trans. Image Process.* 8 (11), 1990, 1572–1585.
  29. Haralick, R.M., Shanmugam, K.K., Dinstein, I., "Texture features for image classification". *IEEE Trans. Syst. Man Cyb.* 8 (6), 1973, 610–621.
  30. Guang-Hai Liu, LeiZhang, "Image retrieval based on multi-texton histogram", *Pattern Recognition* 43 (2010) 2380–2389
  31. Yuanting Gu and Enhua Wu, "Feature Analysis and Texture Synthesis", *IEEE*, 2007, 473-476.

This page is intentionally left blank